Identification of Seven-Gene Hypoxia Signature for Predicting Overall Survival of Hepatocellular Carcinoma

YuPing Bai
Lanzhou University
Wenbo Qi
Lanzhou University
Le Liu
Lanzhou University
Jing Zhang
Lanzhou University Second Hospital
Lan Pang
Lanzhou University Second Hospital
Tiejun Gan
Lanzhou University Second Hospital
Pengfei Wang
Lanzhou University Second Hospital
Hao Chen (ery_chenh@lzu.edu.cn)
Lanzhou University

Research Article

Keywords: HCC, hypoxia, gene signature, prognosis, bioinformatics

Posted Date: December 11th, 2020

DOI: https://doi.org/10.21203/rs.3.rs-121134/v1

Abstract

Background: Hepatocellular carcinoma is ranked fifth among the most common cancer worldwide. Hypoxia can induce tumor growth, but the relationship with HCC prognosis remains unclear. Our study aims to construct a hypoxia-related multigene model to predict the prognosis of HCC.

Methods: RNA-seq expression data and related clinical information were download from TCGA database and ICGC database, respectively. Univariate/multivariate Cox regression analysis was used to construct prognostic models. KM curve analysis, and ROC curve were used to evaluate the prognostic models, which were further verified in the clinical traits and ICGC database. GSEA analyzed pathway enrichment in high-risk groups. Nomogram was constructed to predict the personalized treatment of patients. Finally, real-time fluorescence quantitative PCR(RT-qPCR) was used to detect the expressions of KDELR3 and SCARB1 in normal hepatocytes and 4 hepatocellular carcinoma cells.

Results: Through a series of analyses, 7 prognostic markers related to HCC survival were constructed. HCC patients were divided into the high and low risk group, and the results of KM curve showed that there was a significant difference between the two groups. Stratified analysis found that there were significant differences in risk values of different ages, genders, stages and grades, which could be used as independent predictors. In addition, we assessed the risk value in the clinical traits analysis and found that it could accelerate the progression of cancer, while the results of GSEA enrichment analysis showed that the high-risk group patients were mainly distributed in the cell cycle and other pathways. Then, Nomogram was constructed to predict the overall survival of patients. Finally, RT-qPCR showed that KDELR3 and SCARB1 were highly expressed in HepG2 and L02, respectively.

Conclusion: This study provides a potential diagnostic indicator for HCC patients, and help clinicians to deepen the comprehension in HCC pathogenesis so as to make personalized medical decisions.

1. Introduction

Hepatocellular carcinoma (HCC), characterized by high morbidity and mortality, poses a major challenge to global public health [1]. At the time of diagnosis, most patients have lost the opportunity for curative treatment, including transplantation, resection or ablation. In addition, due to the high recurrence rate, patients receiving potential treatment still have a poor prognosis [2].If patients are at higher risk of recurrence, strict follow-up is required, and patients may also profit from adjuvant therapy after cure, although no adjuvant therapy has hitherto been considered standard treatment[3,4].There has been no consensus on the exploition to predict the prognosis of HCC, though a slew of attempts and efforts have been made. Previous studies have mostly used parametric prediction models constructed with clinical baseline characteristics (such as tumor size, cirrhosis, tumor number, and microvascular infiltration) and single-molecule biomarkers (such as alpha-fetoprotein [AFP] and Des-γ carboxyl-Carboxyl of enzyme) to predict the prognosis of HCC [5].But recently, with the development of genome sequencing technology, the integration of prognostic gene signatures and traditional parameters in the prognosis of HCC has shown

great advantages. Nevertheless, it is still of great necessity to make endeavour for the application of these neoteric genetic propoties in clinical practice.

Hypoxia is one of the markers of tumor microenvironment. Due to insufficient blood supply, growing tumors often occur in a hypoxia state[6].Unlike healthy cells, tumors respond to low oxygen levels by initiating multiple adaptive behaviors (for example, angiogenesis, proliferation, and invasion) that ultimately promote a more aggressive tumor phenotype. For example, glioblastoma can cause extensive tissue hypoxia, which facilitates the induction and maintenance of malignant phenotypes. For the glioma group, tumor hypoxia is associated with anti-apoptosis, tumor recurrence, resistance to chemotherapy and radiotherapy, invasion potential and reduced patient survival [7].In addition, previous studies have shown that nearly 50% of locally advanced breast cancers suffer from hypoxia, leading to failed chemoradiotherapy resistance [8].However, despite considerable efforts on the relationship between hypoxia and tumor, the prediction of the correlation between hypoxic-related gene expression and overall survival rate in HCC patients has not been reported.

In this study, seven hypoxia gene signatures associated with HCC prognosis were constructed using TGCA dataset and validated in the ICGC dataset. Through GSEA functional enrichment analysis, we examined the important role of the prognostic marker gene in the development and progression of HCC. The final results showed that the model had high reliability in predicting the prognosis of HCC patients, and could help clinicians better carry out individualized treatment. After these bioinformatics analyses, two genes not previously reported in HCC, KDELR3 and SCARB1, were selected to study their expression levels in normal hepatocytes L02, hepatocellular carcinoma cells SMMC-7721, HepG2, hu7 and SK-HEP-1, respectively.

2. Materials And Methods

2.1 sample collection

RNAseq data of this sample mainly comes from TCGA cancer database (https://portal.gdc.cancer.gov/) and ICGC international cancer database (https://ICGC.org/), including TGCA dataset as a training set, and ICGC dataset as a verification set. In order to ensure the accuracy and reliability of the data results, the samples with incomplete clinical information and TCGA samples with survival time less than 30 days were eliminated, and finally retained 343 TCGA liver cancer samples and 231 ICGC samples. The 200 hypoxia-related genes were retrieved from Molecular Signatures Database (MSiDb v7.1) and named as HALLMARK_HYPOXIA.

2.2 Prognostic model construction

In order to establish a reliable prognosis signature, we first use Univariate Cox regression analysis, screening of the genes associated with HCC significantly, after using the random forest algorithm for significant genetic screening, and increasing the use of multivariate Cox regression analysis to analyze gene sets, establish related prognosis signature, risk formula is as follows: risk formula = $\sum$

$Coef_{gene}xExp_{genes}$, including $Coef_{gene}$ represent each gene prognosis factor, prognosis of Exp_{genes} represents each gene expression. In each HCC patient, the risk scores of the training set and validation set were calculated based on the risk formula, and under the conditionn of the median value of the risk value, the patients were divided into high-risk and low-risk groups.

2.3 Prognostic model evaluation

Kaplan-Meier (KM) curve was used to analyze and compare the suevival differences between the high-risk and low-risk groups in the prognostic model. Then, ROC curve was used to evaluate the specificity and sensitivity of the prognostic model.In addition, the KM curve was also used to assess the association between prognostic model risk values and clinical traits.To further assess whether the prognostic model could be used as an independent predictor, univariate and multivariate Cox regression analyses were used to evaluate clinical traits and risk values in training sets and external validation sets, and it was found that the prognostic model could be used as an independent predictor. Furthermore, we constructed a nomogram and calibration curve related to these independent predictors for personalized independent survival prediction.

2.4 GSEA enrichment analysis

In order to assess the metabolic pathways involved in the prognostic model, we used GSEA enrichment analysis to assess the enrichment pathways of patients in the high-risk and low-risk groups. We are going to use c2.cp.kegg.v7.1.symbols.gmt as background. The screening of significant pathways was considered to be statistically significant with pValue <0.05 and error discovery rate FDR<0.05.

2.5. Cell culture

Human normal cell line L02, HCC cell lines SMMC-7721, Hep G2, hu7 and SK-HEP-1 were purchased from Cell Resource Center□PMUC (Beijing China). All cells were maintained in Dulbecco's modified Eagle's medium (DMEM; Gibco, USA) supplemented with 10% foetal bovine serum (FBS; Gibco), 1% penicillin and streptomycin (Gibco). The cells were cultured in a 5% CO2-humidified atmosphere at 37℃.

2.6 RNA extraction, reverse-transcription RNA, and quantitative real-time polymerase chain reaction

The total RNA was extracted from cell lines by using the TRIzol reagent (Invitrogen), reverse transcription was performed by using the PrimeScript RT reagent Kit (Takara, Japan) and cDNA was synthesized according to the manufacturer's instructions. The qPCR assay was performed by LightCycler480 system (Roche, Switzerland) and SYBR Green (Takara).

SCARB1: Primer name(F): GGAGATCCCATCCCCTTCTAT, Primer name(R): CTGAACTCCCTGTACACGTAG.

KDELR3: Primer name(F): GAGGCTGAGACCATAACTACTC, Primer name(R)□ AGAAATTCTCAGTCTGGTACCG.

2.7 Statistical method

Statistical software SPSS 20.0 was used for data analysis. Student t test and analysis of variance were used to compare different groups. P< 0.05 was considered statistically significant.

3. Results

3.1 Establishment and validation of hypoxia-related prognostic models

343 patients with liver cancer and 200 genes associated with hypoxia were used to identify the prognostic model.Using univariate cox regression analysis, 79 survival-related hypoxic genes were selected forst and then the random forest algorithm was used for feature selection. We identified the genes of the relative importanct gene>0.4 was identified as the final feature (Figure 1A-B). In view of these characteristics, we used multivariate Cox regression analysis to construct the prognosis model containing 7 hypoxic gene-related genes. Through the correlation coefficient, the risk formula was constructed, as follows: r risk score = LDHA * 0.000812695+ KDELR3 * 0.000649537+ CDKN1C * 0.002057653+ SLC2A1 * 0.004190531+ NDRG1 * 0.001235623+ VHL * 0.023669962+SCARB1* 0.00060351.Through the risk formula, the risk values of each patient in the training set and external validation set were calculated, and the patients were further divided into high-risk group and low-risk group on the basis of the median risk value. We found the number of death toll from the high-risk group of patients is significantly higher than low-risk group (Figure2A-B), moreover, the KM curve analysis that according to the results of the survival of high and low risk group has obvious differences, the survival rate of patients with low risk is far higher than the risk group (P < 0.05) (Figure3A-B), in addition, the results show that the training sample set and validation set outside the ROC curve prognosis is of high accuracy (Figure 3C-D).

3.2 Independent assessment of prognostic model

To assess the prognostic independence of this prognostic model in both the training set and the validation set samples, we first retained clinical traits (age, sex, stage, and grade) that existed in both data sets. Using univariate and multivariate cox regression analyses, we found that the prognostic model was significant in both data sets, suggesting that the prognostic model could act as an independent prognostic factor (Figure4).

3.3 Association between prognostic models and clinical cause groups

In order to explore the association between prognostic models and clinical traits, we first assessed the distribution of risk values in clinical traits and found that risk values for G3-4 were significantly higher than G1-2 (P<0.05). In addition, the risk values for stage Stage III-IV were significantly higher than that of Stage I-II. These results suggest that a higher risk score is associated with a higher degree of HCC malignancy(Figure5).

Therefore, this prognostic model can accurately predict the progression of HCC. In addition, in order to study the prognostic value of the model stratified by clinicopathological variables for HCC patients, stratified analysis was conducted for HCC patients according to age, sex, grade, and stage. For all the different stratifications, the Overall Survival (OS) time was significantly shorter in the high-risk group than in the low-risk group (Figure 6). These results suggest that the prognostic model can predict the prognosis of HCC patients without considering clinicopathological variables.

3.4 The construction and verification of nomogram in TCGA data set and ICGC data set

In order to establish quantitative prognostic methods for HCC, normogram was established by independent prognostic factors and prognostic models of two data sets. Based on multivariate Cox analysis, point ratios in nomogram were used to assign points. We drew a horizontal line to determine the points for each variable, calculated the total points for each patient by adding the points for all variables, and normalized it to a distribution of 0 to 100. By drawing a vertical line between the total point axis and each pre-posterior axis, we can calculate the estimated 1-year,3-year and 5-year survival rates of HCC patients, which may be helpful for practitioners to conduce clinical decisions about the prognosis of HCC patients. In addition, we evaluated the accuracy and consistency of the nomo diagram by performing the ROC curve and the calibration curve respectively (Figure 7).

3.5 Functional enrichment analysis of prognostic model

In order to further explore the potential function and role of prognostic models in HCC, GSEA enrichment analysis was used for enrichment analysis of high and low risk groups. The results showed the cell cycle, MTOR signaling pathways, OOCYTEMEIOSIS and UBIQUITINMEDIATESPROTEOLYSIS pathway were significantly enriched in the high-risk group (Figure 8).

3.6 Expression levels of kdelr3 and SCARB1

To better explain the biological function of these genes in the pathogenesis and development of HCC, we selected two genes not reported in HCC studies for RT-qPCR to study the differences in their expression levels. We found that the expression of KDELR3 was the highest in G2, while the lowest in 7721, L02 was the highest in SCARB1, and SK-HEP-1 was the lowest ($p < 0.05$) (Figure 9).

4. Discussion

Hepatocellular carcinoma (HCC) is one of the major health threats around the world, particularly in East Asia. Even after radical resection, the long-term outcome of HCC patients remains depressed [9].Therefore, it is very important to develop a prognostic model suitable for HCC patients. Recently, with the improvement of genome sequencing, biochip and high-throughput sequencing technologies, more and more studies have applied bioinformatics methods to chip dataset analysis, which provides an effective new method for the diagnosis, treatment and prognosis of HCC. In this study, a total of 574 HCC samples were downloaded from TCGA and ICGC databases, using TCGA as the training set and ICGC as the test

set. Through bioinformatics analysis, a prognostic model of HCC with 7 genes associated with hypoxia was constructed for the first time. Our prognostic model can effectively stratify the survival of patients. We found the efficacy of our prognostic model in both the training set and the external validation set, suggesting that the model has strong prognostic value. In addition, the prognostic model showed a significant correlation with clinicopathological factors, further supporting the robustness of the prognostic role of our model. In addition, univariate and multivariate Cox regression analysis were used to validate our prognostic model as an independent predictor. Nomogram of independent predictors (staging and prognostic models) were constructed and showed that the model performed well in predicting 1-year, 3-year, and 5-year OS, which may be useful for planning short-term follow-up for individual treatment. In summary, the predictive prognostic value of our signatures is greatly reflected in these results, but it is worth noting that only two databases were selected. To validate the model on a large scale, the signatures need to be validated in a more independent queue.

Among the seven genes in the prognostic model that we constructed, LDHA (lactate dehydrogenase A) is A crucial REDOX enzyme in the glycolysis pathway in organisms, which can reversely catalyze the oxidation of lactic acid to pyruvate, and this catalytic reaction is the final product of anaerobic glycolysis [10].In addition, LDHA can be used as a possible prognostic marker for lung adenocarcinoma survival, and the high expression of LDHA is associated with poor prognosis[11]. NDRG1 is a known metastasis inhibitor in a variety of cancers, participating in embryogenesis, cell growth, lipid biosynesis, stress response, and immunity. During metastasis, tumor growth and invasion require angiogenesis, and overexpression of NDRG1 is associated with a decrease in pro-angiogenic factors, resulting in a decrease of angiogenesis in pancreatic cancer [12].The expression levels of NDRG2 and LDHA are closely related to the prognosis of HCC patients and can be used as prognostic markers [13].KDELR3 is the third confirmed member in the KDEL family,which encodes proteins associated with the endoplasmic reticulum (ER). Reports have shown previously that KDELR3 expression in arteriosclerosis macrophages could be obviously differ from that in non-arteriosclerosis tissues, and the higher expression level in non-arteriosclerosis tissues, which can be used as a potential prognostic factor [14]. CDKN1C, DKN1C, also known as p57Kip2, are cyclin-dependent kinase inhibitors. The gene encoding CDKN1C is located on chromosome 11p15.5.CDKN1C belongs to the kinase inhibitor protein /CDK interacting protein (Kip/Cip) family, which consists of three members, namely CDKN1A/p21Cip1, CDKN1B/p27Kip1 and CDKN1C/p57Kip2.Previously, CDKN1C was identified as a tumor suppressor gene with decreased expression in various cancers including hepatocellular carcinoma, colorectal cancer and ovarian cancer [15].Thus, upregulation of CDKN1C leads to inhibition of markers involved in cell growth, differentiation, cell death, and angiogenesis in malignant tumors.SLC2A1 has been extensively studied as a major glucose transporter and has been identified as a possible prognostic factor for several cancers, including HCC and NSCLC et al [16].The absence of von Hippel-Lindau (VHL), a tumor suppressor gene, is a hallmark of clear cell renal carcinoma. In addition, VHL inactivation leads to constitutive activation of hypoxia-inducing factor (HIF) HIF-1 and HIF-2 and their downstream targets (including pro-angiogenic factors VEGF and PDGF), while the activation of HIF and its downstream targets induces tumor formation [17].SCARB1 (Scavenger receptor class B member 1;) is a protein-coding gene. The related pathways

include lipoprotein metabolism and folic acid metabolism.Studies have also found that SCARB1 can be a potential target for prostate cancer [18].

The relationship between cell cycle and malignancy is now fully established, and our GSEA results show that the associated pathways are enriched in high-risk patients. The activation of mTOR related pathways can promote the vitality and motility of HCC cell lines [19]. Enrichment of The OOCYTEMEIOSIS pathway was found in bladder cancer and cervical cancer [20,21].UBIQUITINMEDIATESPROTEOLYSIS related pathways plays an important role in the disease progression of colorectal cancer and non-small cell lung cancer [22, 23].These three pathways were enriched in our high-risk patient group.

Although we have made a lot of efforts to study the prognostic model, there are still many defects. The clinical information of external validation set and test set is not fully matched, leading to the omission of partial clinical information and the inability to fully understand the correlation between the prognostic model and clinical practice.Moreover, none of genes have been verified, because some of them have been studied in HCC. In view of this, two genes, KDELR3 and SCARB1, have not been studied in HCC, laying a foundation for further studies in the future.

In conclusion, a prognostic model consists of 7 genes associated with hypoxia was constructed to provide potential biomarkers for the prognosis of HCC ,which contributed to the understanding of the underlying HCC pathogenesis.

Declarations

Acknowledgements

We thanked Hao Chen of lanzhou University for Project design.

Authors' contributions

CH and BYP conceived of the study and participated in design and coordination, drafted and revised the manuscript. QWB□ll and ZJ performed gene differential analysis and survival analysis using GEO and TCGA data. PL and GTJ collected and analyze PCR related information. WPF and CH revised manuscript. All authors read and approved the final manuscript.

Funding

This study was supported by Key Project of Science and Technology in Gansu province(19ZD2WA001) and Cuiying Scientific and Technological Innovation Program of Lanzhou University Second Hospital (No. CY2017-ZD01)

Competing interests

The authors declare that they have no competing interests.

Availability of data and materials

All data generated or analysed during this study are included in this published article.

Ethics approval and consent to participate

Not applicable.

Consent for publication

Not applicable.

Abbreviations

TCGA The Cancer Genome Atlas

ICGC International Cancer Genome Consortium

KM Kaplan–Meier

qRT-PCR quantitative reverse transcription polymerase chain reaction

HCC hepatocellular carcinoma

GSEA gene set enrichment analysis

ROC receiver operating characteristic

References

1. El-Serag H. B. (2011). Hepatocellular carcinoma. The New England journal of medicine, 365(12), 1118–1127.
2. Yang, J. D., Hainaut, P., Gores, G. J., Amadou, A., Plymoth, A., & Roberts, L. R. (2019). A global view of hepatocellular carcinoma: trends, risk, prevention and management. Nature reviews. Gastroenterology & hepatology, 16(10), 589–604.
3. França, A. V., Elias Junior, J., Lima, B. L., Martinelli, A. L., & Carrilho, F. J. (2004). Diagnosis, staging and treatment of hepatocellular carcinoma. Brazilian journal of medical and biological research = Revista brasileira de pesquisas medicas e biologicas, 37(11), 1689–1705.
4. Wang, J., He, X. D., Yao, N., Liang, W. J., & Zhang, Y. C. (2013). A meta-analysis of adjuvant therapy after potentially curative treatment for hepatocellular carcinoma. Canadian journal of gastroenterology = Journal canadien de gastroenterologie, 27(6), 351–363.
5. AlSalloom A. A. (2016). An update of biochemical markers of hepatocellular carcinoma. International journal of health sciences, 10(1), 121–136.

6. Lou J, Zhang L, Lv S, Zhang C, Jiang S. Biomarkers for Hepatocellular Carcinoma. Biomark Cancer. 2017;9:1-9. Published 2017 Feb 28. doi:10.1177/1179299X16684640
7. D'Alessio, A., Proietti, G., Sica, G., & Scicchitano, B. M. (2019). Pathological and Molecular Features of Glioblastoma and Its Peritumoral Tissue. Cancers, 11(4), 469.
8. Vaupel, P., Briest, S., & Höckel, M. (2002). Hypoxia in breast cancer: pathogenesis, characterization and biological/therapeutic implications. Wiener medizinische Wochenschrift (1946), 152(13-14), 334–342. https://doi.org/10.1046/j.1563-258x.2002.02032.x
9. Mazzanti, R., Arena, U., & Tassi, R. (2016). Hepatocellular carcinoma: Where are we? World journal of experimental medicine, 6(1), 21–36.
10. Guo, Y., Li, X., Sun, X., Wang, J., Yang, X., Zhou, X., Liu, X., Liu, W., Yuan, J., Yao, L., Li, X., & Shen, L. (2019). Combined Aberrant Expression of NDRG2 and LDHA Predicts Hepatocellular Carcinoma Prognosis and Mediates the Anti-tumor Effect of Gemcitabine. International journal of biological sciences, 15(9), 1771–1786.
11. Yu, X., Zhang, X., & Zhang, Y. (2020). Identification of a 5-Gene Metabolic Signature for Predicting Prognosis Based on an Integrated Analysis of Tumor Microenvironment in Lung Adenocarcinoma. Journal of oncology, 2020, 5310793.
12. Hosoi, F., Izumi, H., Kawahara, A., Murakami, Y., Kinoshita, H., Kage, M., Nishio, K., Kohno, K., Kuwano, M., & Ono, M. (2009). N-myc downstream regulated gene 1/Cap43 suppresses tumor growth and angiogenesis of pancreatic cancer through attenuation of inhibitor of kappaB kinase beta expression. Cancer research, 69(12), 4983–4991.
13. Guo, Y., Li, X., Sun, X., Wang, J., Yang, X., Zhou, X., Liu, X., Liu, W., Yuan, J., Yao, L., Li, X., & Shen, L. (2019). Combined Aberrant Expression of NDRG2 and LDHA Predicts Hepatocellular Carcinoma Prognosis and Mediates the Anti-tumor Effect of Gemcitabine. International journal of biological sciences, 15(9), 1771–1786.
14. Huang, H. M., Jiang, X., Hao, M. L., Shan, M. J., Qiu, Y., Hu, G. F., Wang, Q., Yu, Z. Q., Meng, L. B., & Zou, Y. Y. (2019). Identification of biomarkers in macrophages of atherosclerosis by microarray analysis. Lipids in health and disease, 18(1), 107.
15. Peng, Y. T., Wu, W. R., Chen, L. R., Kuo, K. K., Tsai, C. H., Huang, Y. T., Lan, Y. H., Chang, F. R., Wu, Y. C., & Shiue, Y. L. (2015). Upregulation of cyclin-dependent kinase inhibitors CDKN1B and CDKN1C in hepatocellular carcinoma-derived cells via goniothalamin-mediated protein stabilization and epigenetic modifications. Toxicology reports, 2, 322–332.
16. Shang, R., Wang, M., Dai, B., Du, J., Wang, J., Liu, Z., Qu, S., Yang, X., Liu, J., Xia, C., Wang, L., Wang, D., & Li, Y. (2020). Long noncoding RNA SLC2A1-AS1 regulates aerobic glycolysis and progression in hepatocellular carcinoma via inhibiting the STAT3/FOXM1/GLUT1 pathway. Molecular oncology, 14(6), 1381–1396.
17. Gossage, L., Eisen, T., & Maher, E. R. (2015). VHL, the story of a tumour suppressor gene. Nature reviews. Cancer, 15(1), 55–64.

18. Gordon, J. A., Noble, J. W., Midha, A., Derakhshan, F., Wang, G., Adomat, H. H., Tomlinson Guns, E. S., Lin, Y. Y., Ren, S., Collins, C. C., Nelson, P. S., Morrissey, C., Wasan, K. M., & Cox, M. E. (2019). Upregulation of Scavenger Receptor B1 Is Required for Steroidogenic and Nonsteroidogenic Cholesterol Metabolism in Prostate Cancer. Cancer research, 79(13), 3320–3331.
19. Wu, T., Dong, X., Yu, D., Shen, Z., Yu, J., & Yan, S. (2018). Natural product pectolinarigenin inhibits proliferation, induces apoptosis, and causes G2/M phase arrest of HCC via PI3K/AKT/mTOR/ERK signaling pathway. OncoTargets and therapy, 11, 8633–8642.
20. Gao, X., Chen, Y., Chen, M., Wang, S., Wen, X., & Zhang, S. (2018). Identification of key candidate genes and biological pathways in bladder cancer. PeerJ, 6, e6036.
21. Wu, X., Peng, L., Zhang, Y., Chen, S., Lei, Q., Li, G., & Zhang, C. (2019). Identification of Key Genes and Pathways in Cervical Cancer by Bioinformatics Analysis. International journal of medical sciences, 16(6), 800–812.
22. Wu, D. M., Deng, S. H., Zhou, J., Han, R., Liu, T., Zhang, T., Li, J., Chen, J. P., & Xu, Y. (2020). PLEK2 mediates metastasis and vascular invasion via the ubiquitin-dependent degradation of SHIP2 in non-small cell lung cancer. International journal of cancer, 146(9), 2563–2575.
23. Lu, J., Li, Y., Wu, Y., Zhou, S., Duan, C., Dong, Z., Kang, T., & Tang, F. (2018). MICAL2 Mediates p53 Ubiquitin Degradation through Oxidating p53 Methionine 40 and 160 and Promotes Colorectal Cancer Malignance. Theranostics, 8(19), 5289–5306.

Figures

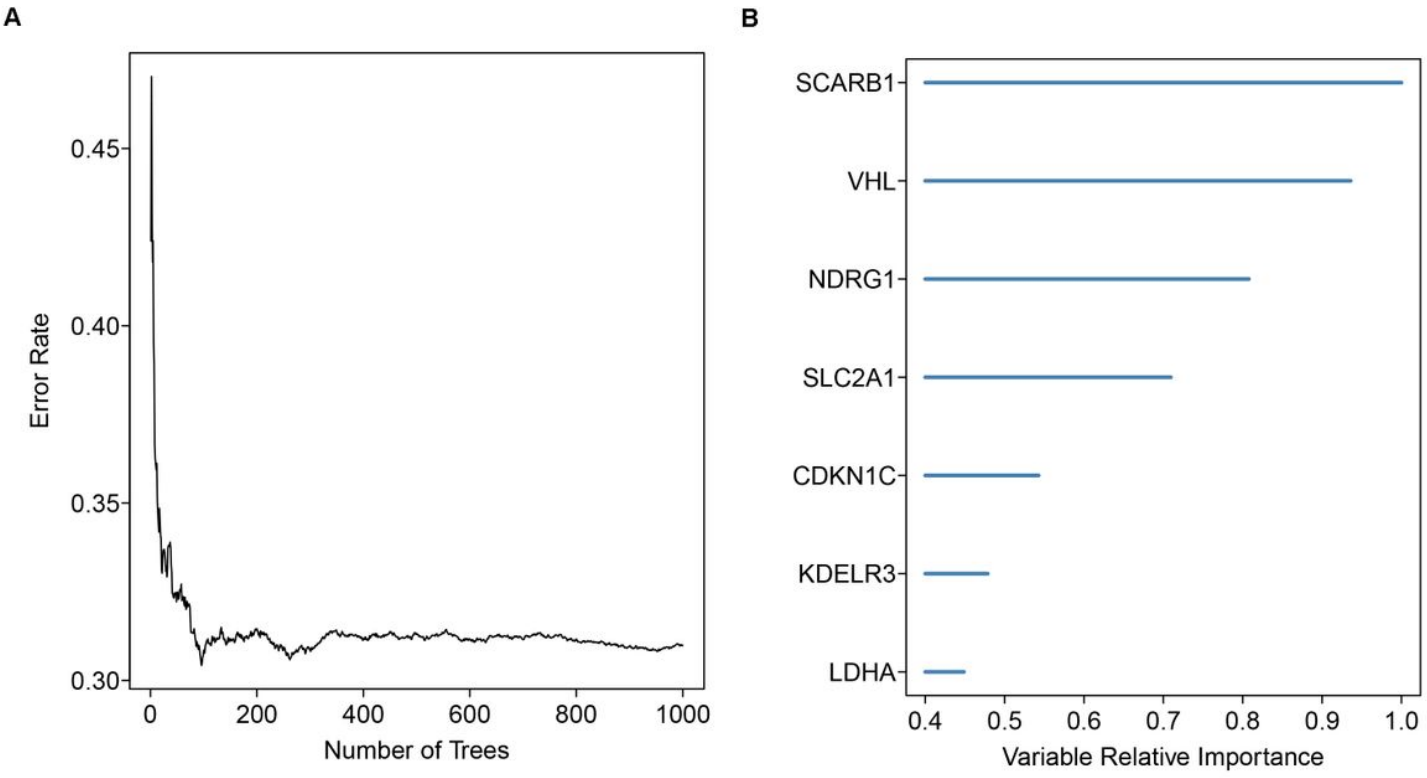

Figure 1

Gene signature selection using the forest analysis. (A) The distribution of the error rate (B) Signature gene importance values for the predictors in the HCC.

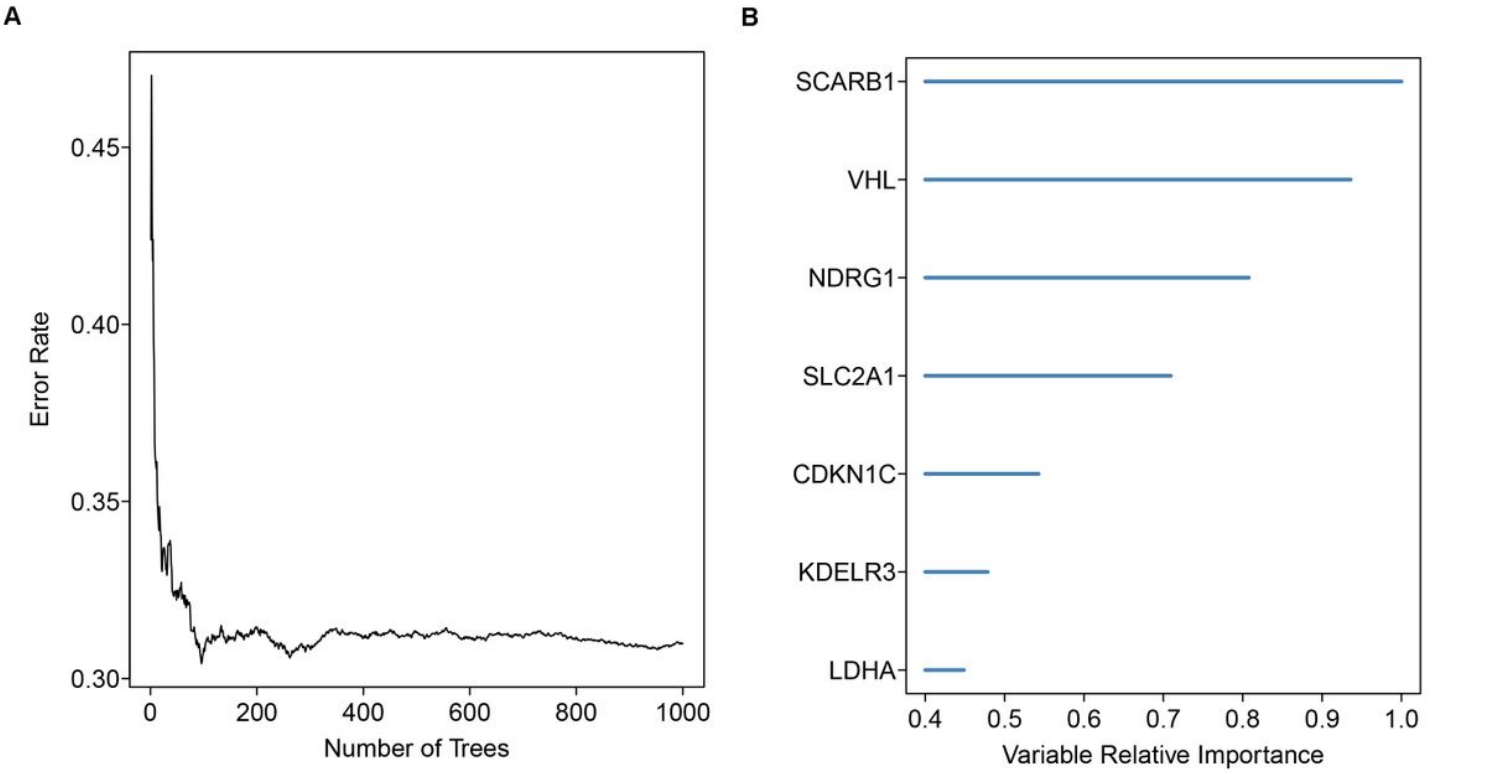

Figure 1

Gene signature selection using the forest analysis. (A) The distribution of the error rate (B) Signature gene importance values for the predictors in the HCC.

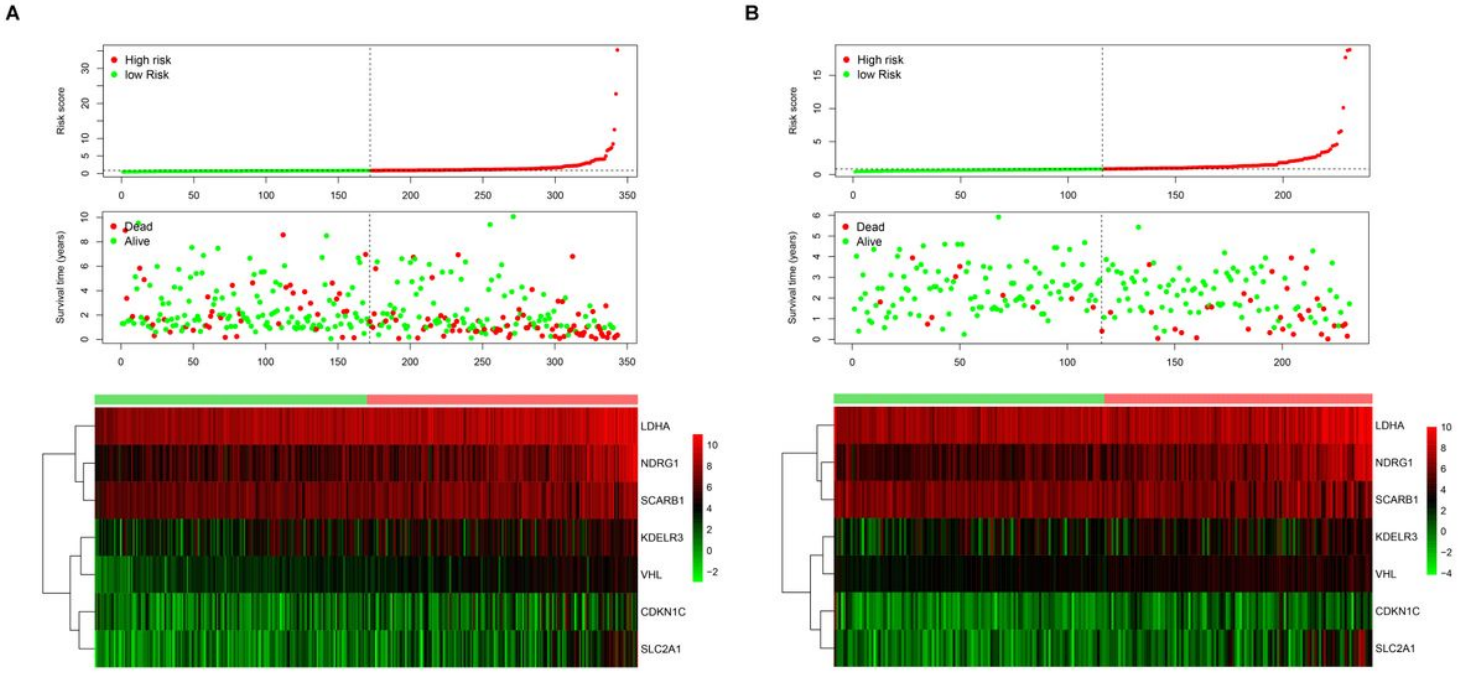

Figure 2

The characteristic of prognostic gene signature in the training dataset (A) and external validation dataset (B). The upper panel represent the risk score distribution, the middle panel is the cases distribution and the lower panel is prognostic gene expression.

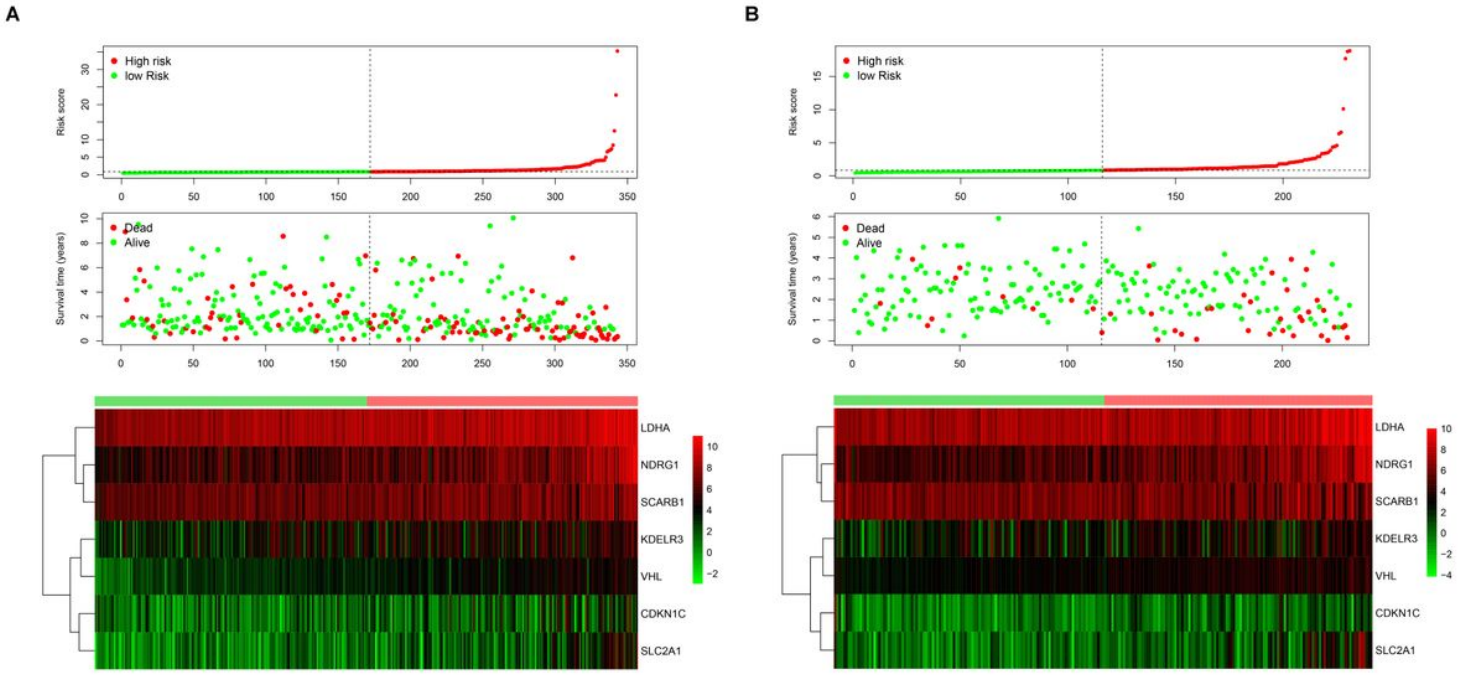

Figure 2

The characteristic of prognostic gene signature in the training dataset (A) and external validation dataset (B). The upper panel represent the risk score distribution, the middle panel is the cases distribution and the lower panel is prognostic gene expression.

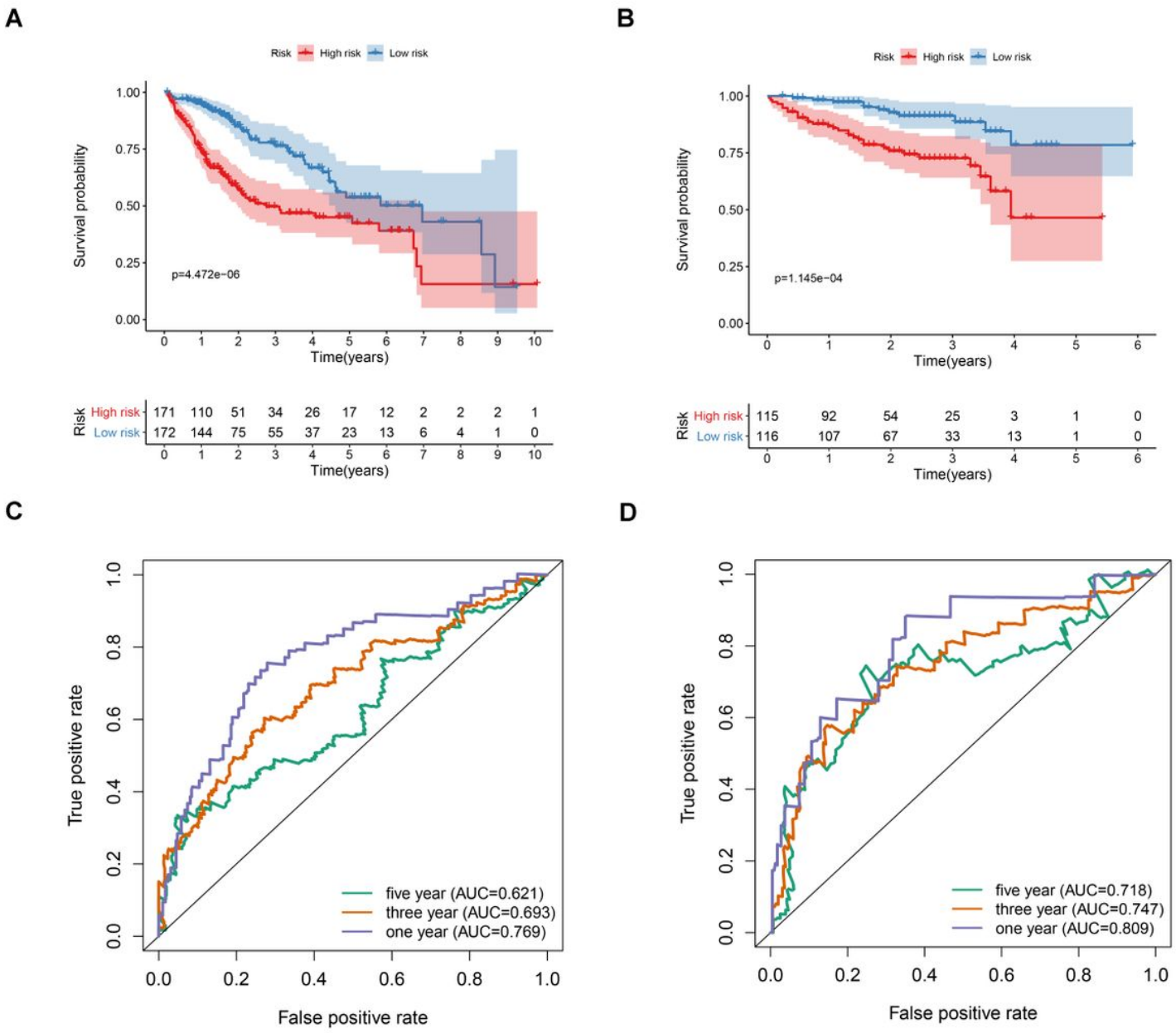

Figure 3

Prognostic value of the hypoxia risk signature in HCC. (A) Kaplan-Meier curve analysis of the hypoxia risk signature in the TCGA dataset. (B) Kaplan-Meier curve analysis of the hypoxia risk signature in the ICGC dataset. (C) ROC curve analysis of the hypoxia risk signature of the 1-, 3-, 5-year in the TCGA dataset. (D) ROC curve analysis of the hypoxia risk signature of the 1-, 3-, 5-year in the ICGC dataset.

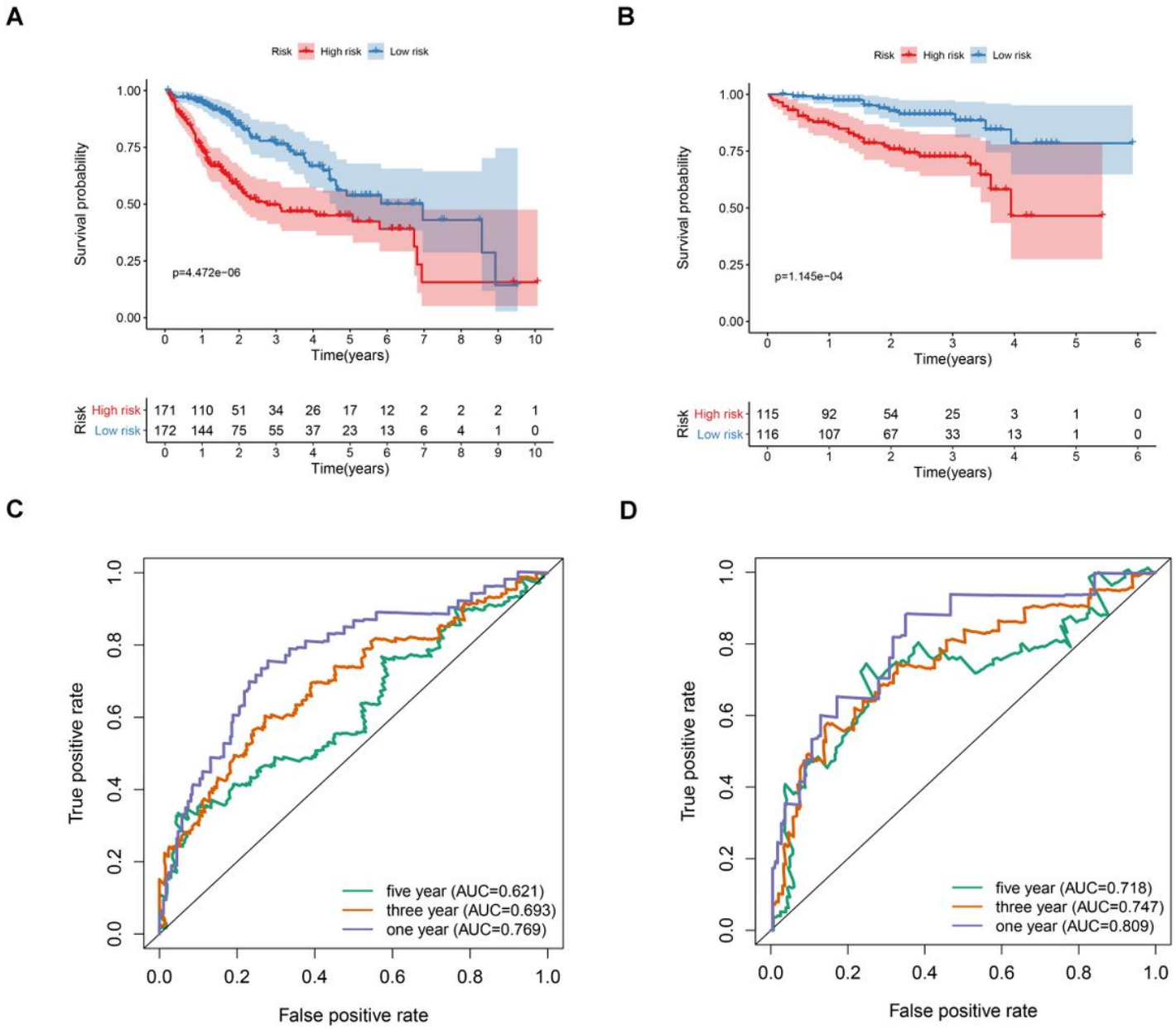

Figure 3

Prognostic value of the hypoxia risk signature in HCC. (A) Kaplan-Meier curve analysis of the hypoxia risk signature in the TCGA dataset. (B) Kaplan-Meier curve analysis of the hypoxia risk signature in the ICGC dataset. (C) ROC curve analysis of the hypoxia risk signature of the 1-, 3-, 5-year in the TCGA dataset. (D) ROC curve analysis of the hypoxia risk signature of the 1-, 3-, 5-year in the ICGC dataset.

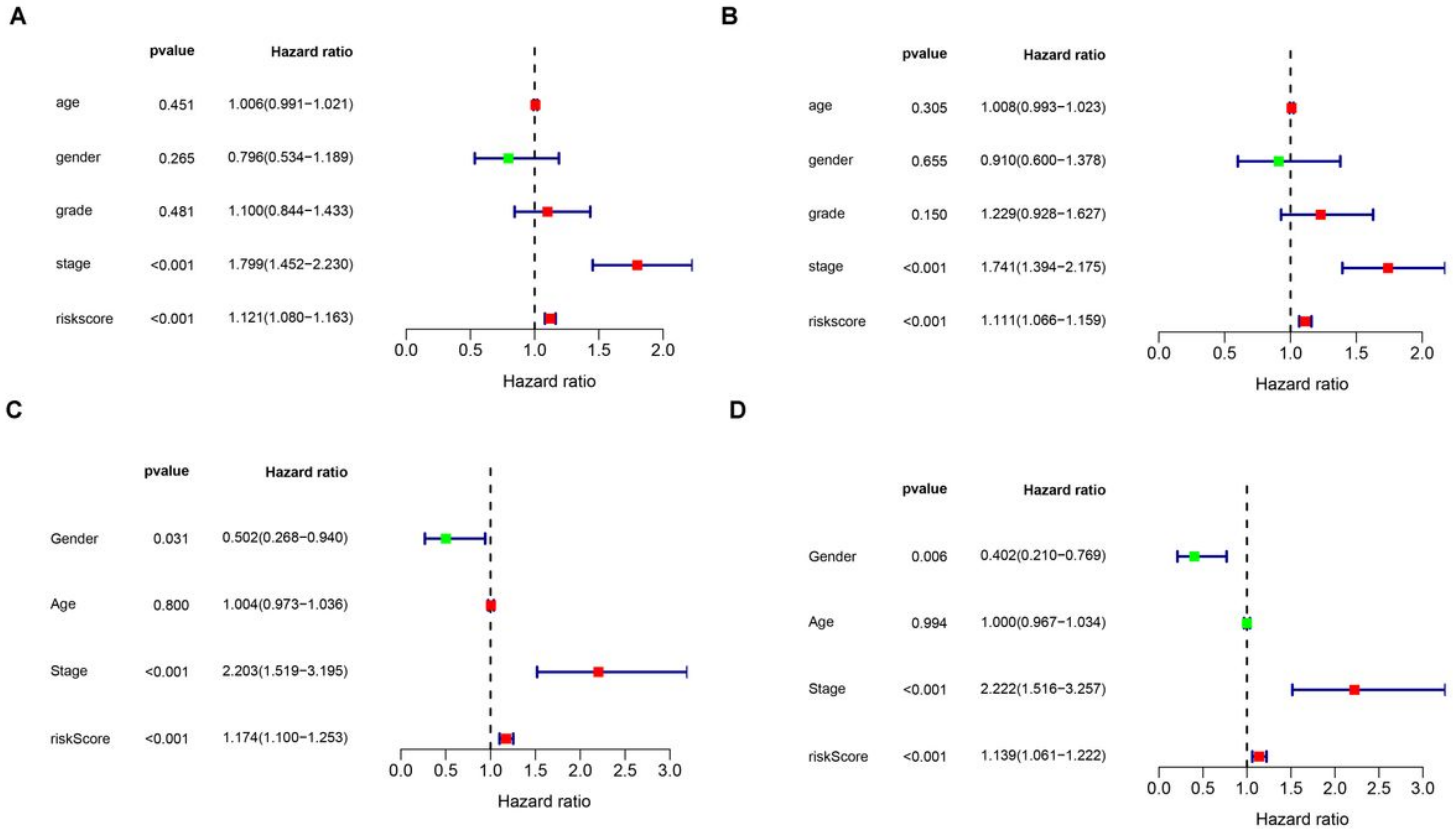

Figure 4

Independence identification of the hypoxia risk signature in the TCGA (A-B) and ICGC (C-D) dataset.

A
pvalue
Hazard ratio
age 0.451 1.006(0.991−1.021)
gender 0.265 0.796(0.534−1.189)
grade 0.481 1.100(0.844−1.433)
stage <0.001 1.799(1.452−2.230)
riskscore <0.001 1.121(1.080−1.163)
0.0 0.5 1.0 1.5 2.0
Hazard ratio
B
pvalue
Hazard ratio
age 0.305 1.008(0.993−1.023)
gender 0.655 0.910(0.600−1.378)
grade 0.150 1.229(0.928−1.627)
stage <0.001 1.741(1.394−2.175)
riskscore <0.001 1.111(1.066−1.159)
0.0 0.5 1.0 1.5 2.0
Hazard ratio
C
pvalue
Hazard ratio
Gender 0.031 0.502(0.268−0.940)
Age 0.800 1.004(0.973−1.036)
Stage <0.001 2.203(1.519−3.195)
riskScore <0.001 1.174(1.100−1.253)
0.0 0.5 1.0 1.5 2.0 2.5 3.0
Hazard ratio
D
pvalue
Hazard ratio
Gender 0.006 0.402(0.210−0.769)
Age 0.994 1.000(0.967−1.034)
Stage <0.001 2.222(1.516−3.257)
riskScore <0.001 1.139(1.061−1.222)
0.0 0.5 1.0 1.5 2.0 2.5 3.0
Hazard ratio

Figure 4

Independence identification of the hypoxia risk signature in the TCGA (A-B) and ICGC (C-D) dataset.

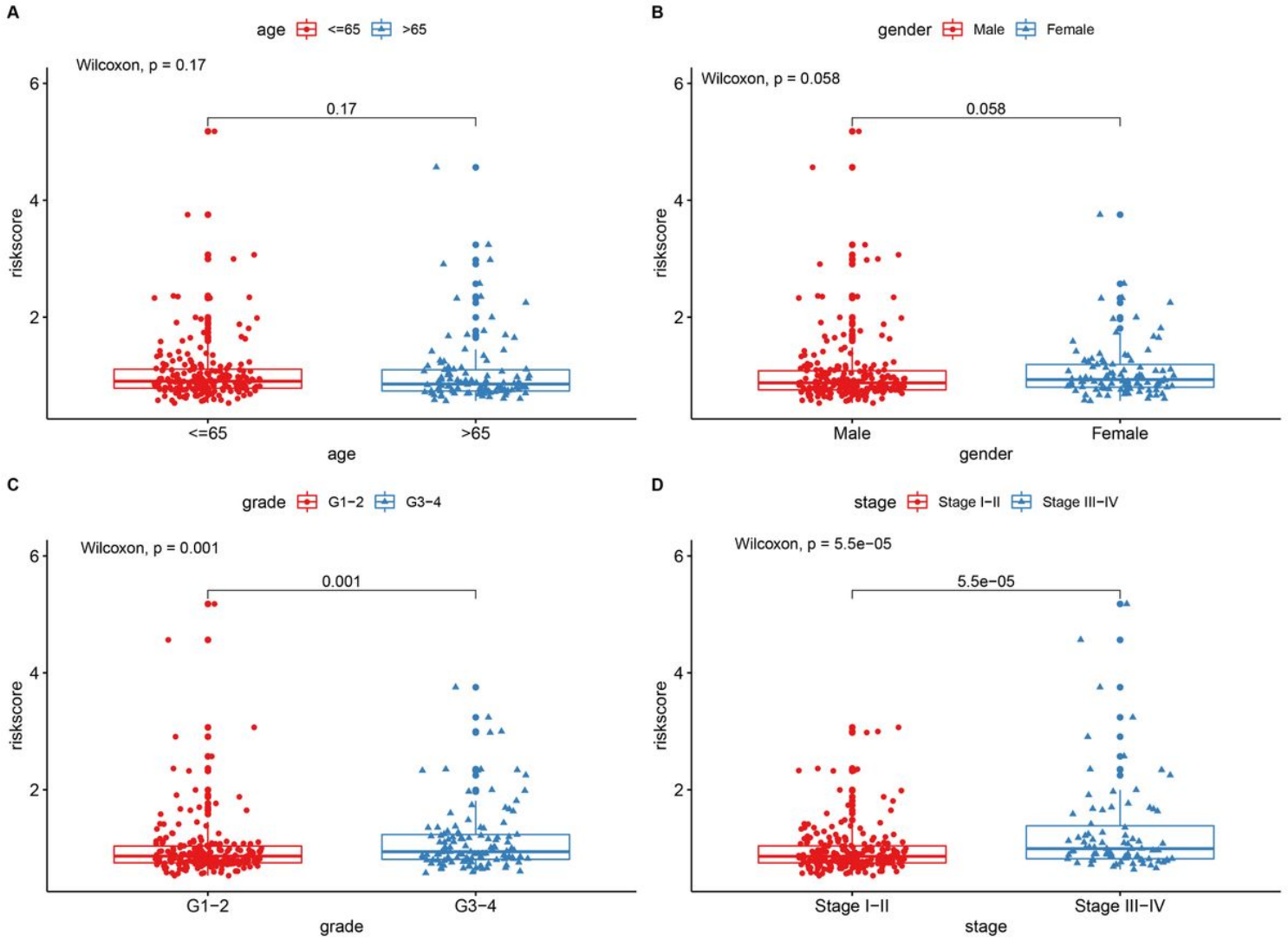

Figure 5

The correlations between the model risk score and clinical factors. (A) Age. (B) Gender. (C) Grade. (D) Stage.

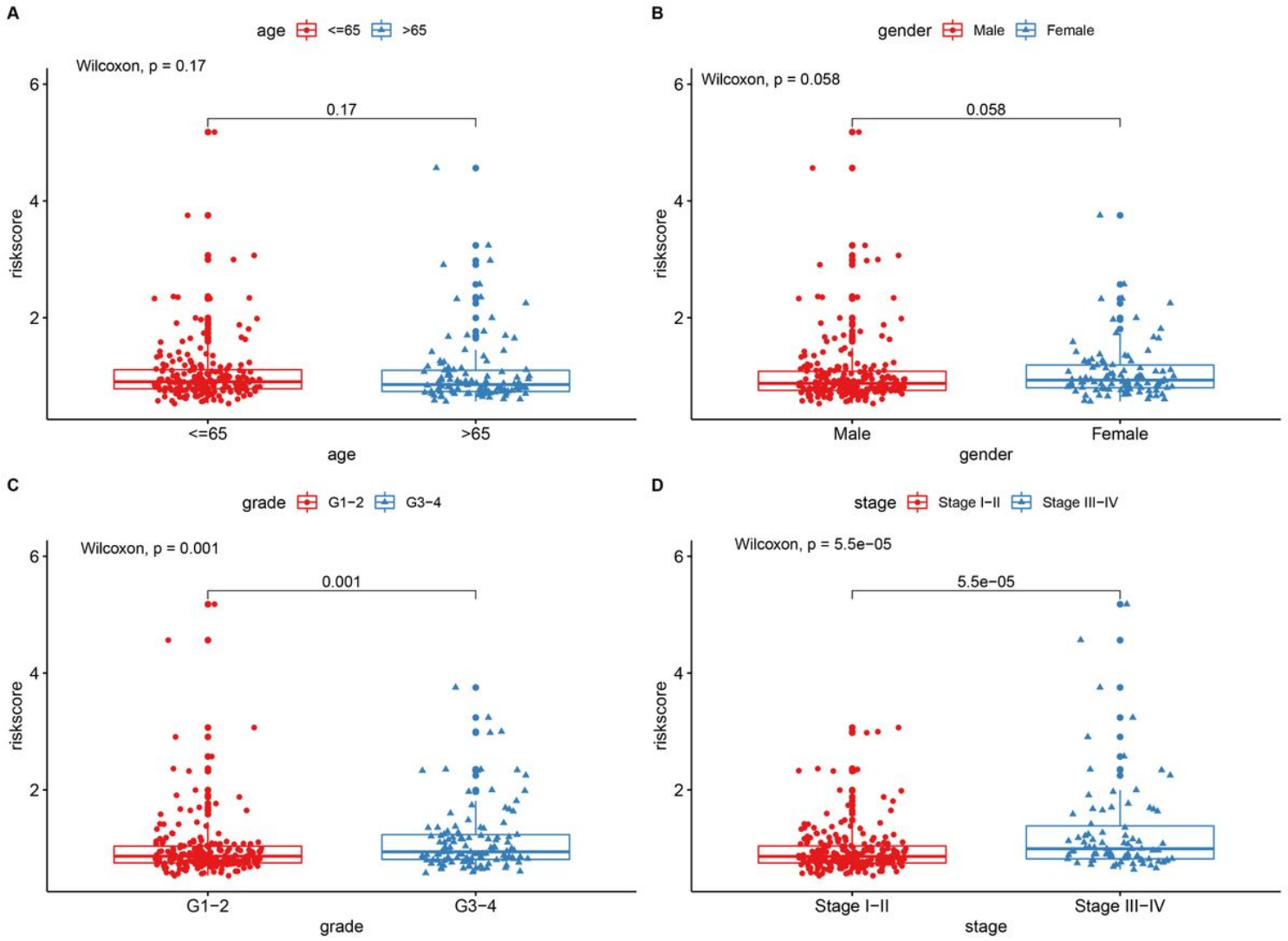

Figure 5

The correlations between the model risk score and clinical factors. (A) Age. (B) Gender. (C) Grade. (D) Stage.

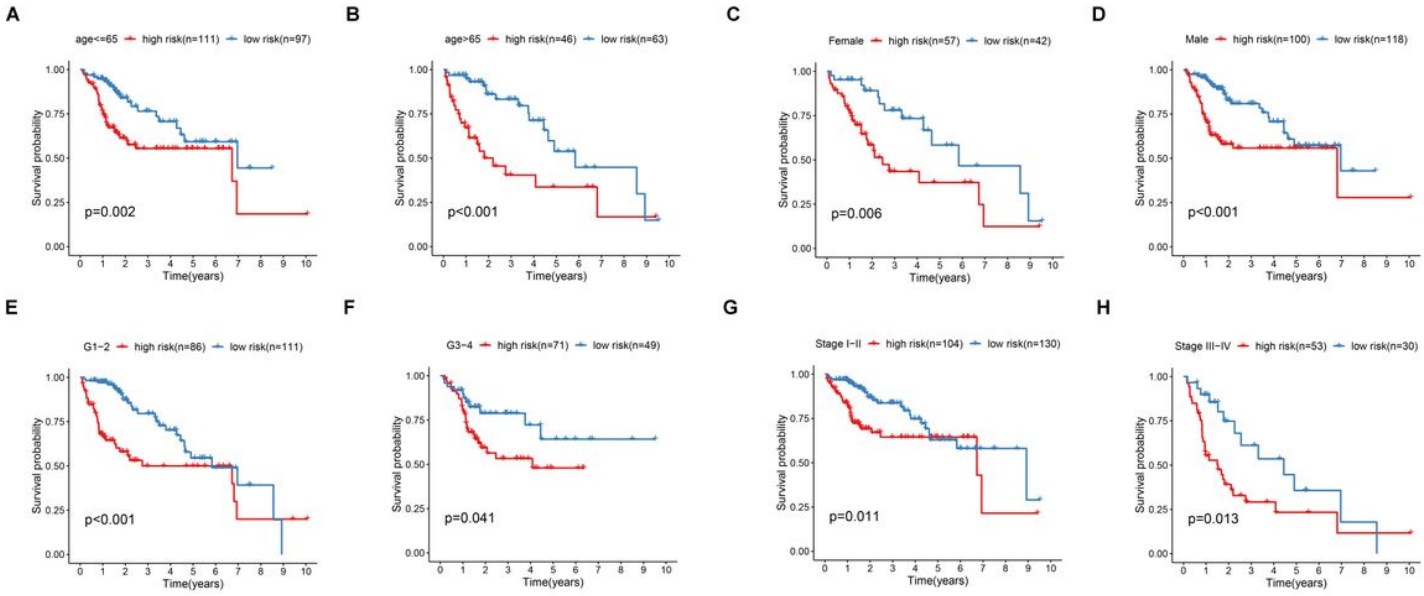

Figure 6

The correlations between the model risk score and clinical factors. (A) Age. (B) Gender. (C) Grade. (D) Stage.

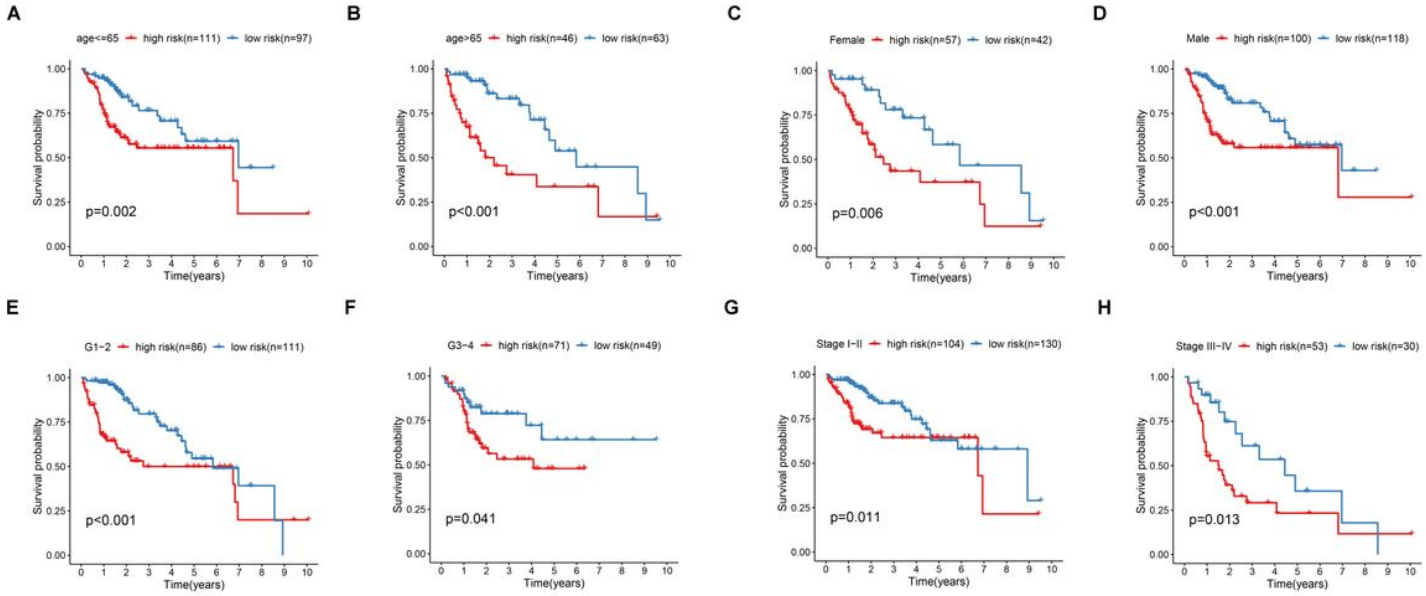

Figure 6

The correlations between the model risk score and clinical factors. (A) Age. (B) Gender. (C) Grade. (D) Stage.

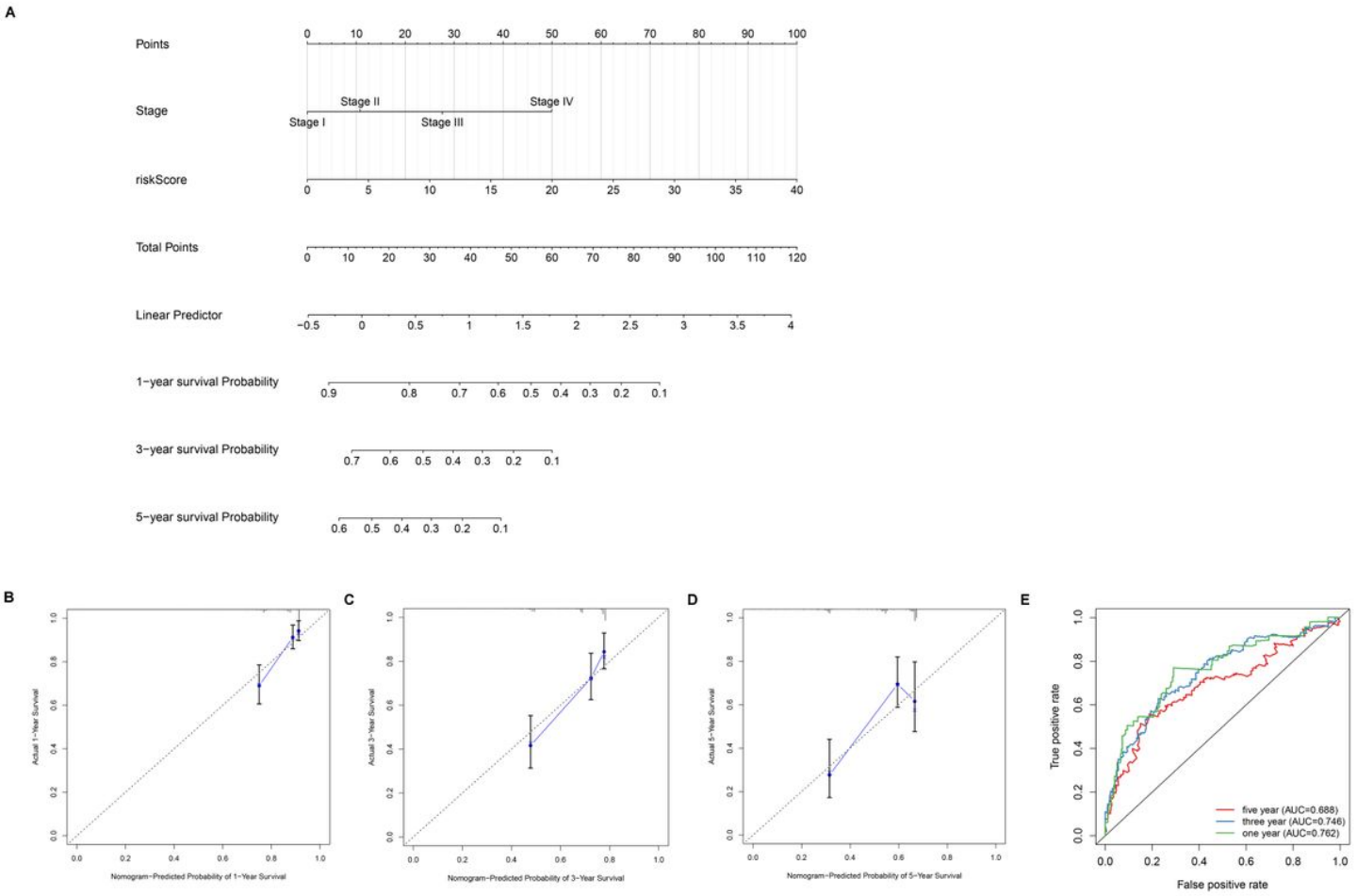

Figure 7

Construction of the nomogram and calibration curve plot. (A) nomogram construction based on the independent clinical factors including stage and risk score. (B) calibration curve plot for predicting 1-year OS in TCGA dataset. (C) calibration curve plot for predicting 3-year OS in TCGA dataset. (D) calibration curve plot for predicting 5-year OS in TCGA dataset. (E) ROC curves analysis of the nomogram in 1-, 3- and 5-year.

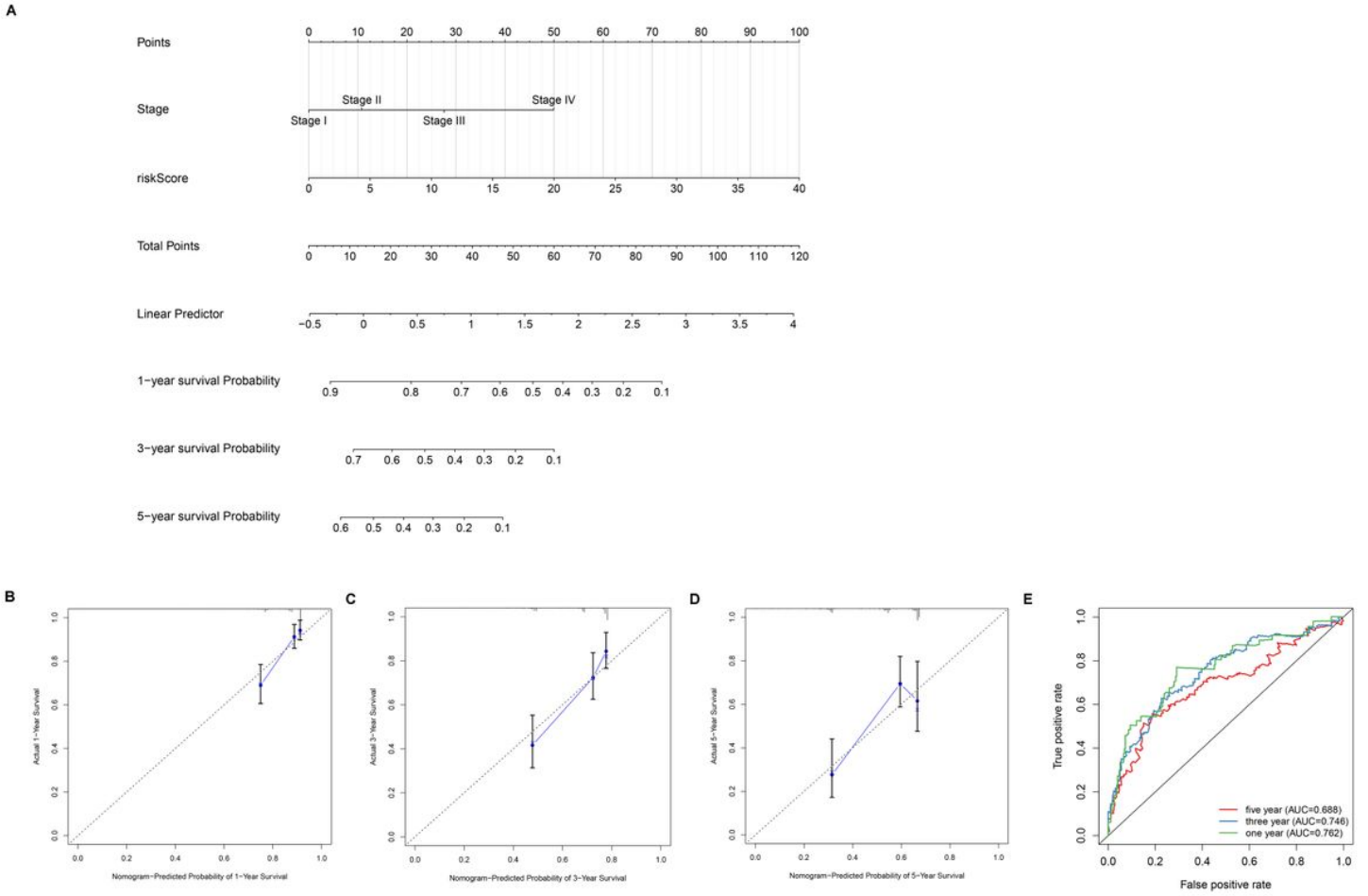

Figure 7

Construction of the nomogram and calibration curve plot. (A) nomogram construction based on the independent clinical factors including stage and risk score. (B) calibration curve plot for predicting 1-year OS in TCGA dataset. (C) calibration curve plot for predicting 3-year OS in TCGA dataset. (D) calibration curve plot for predicting 5-year OS in TCGA dataset. (E) ROC curves analysis of the nomogram in 1-, 3- and 5-year.

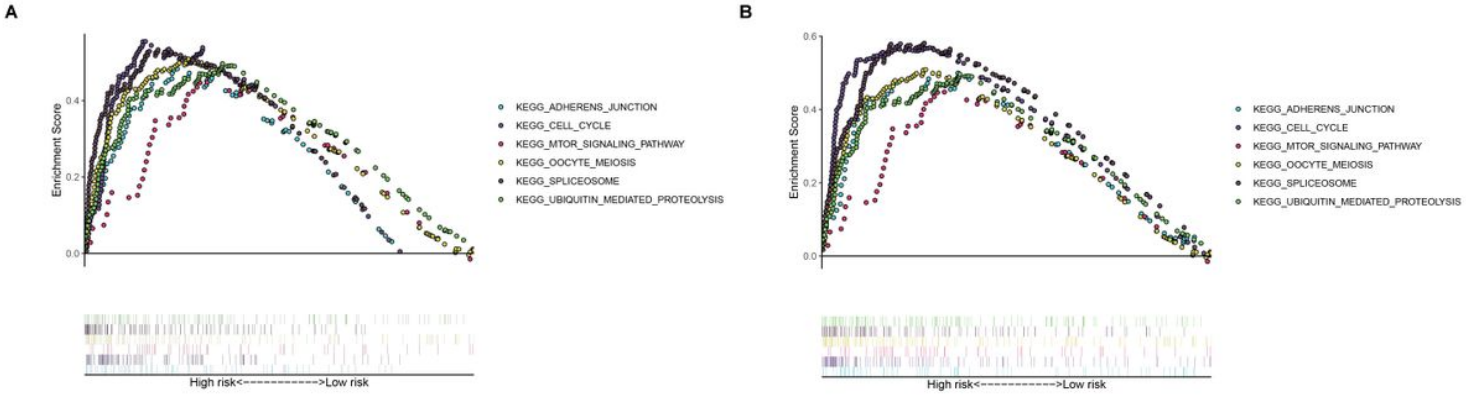

Figure 8

Gene Set Enrichment Analysis of the hypoxia risk signature in the highly risk group of TCGA (A) and ICGC (B) dataset

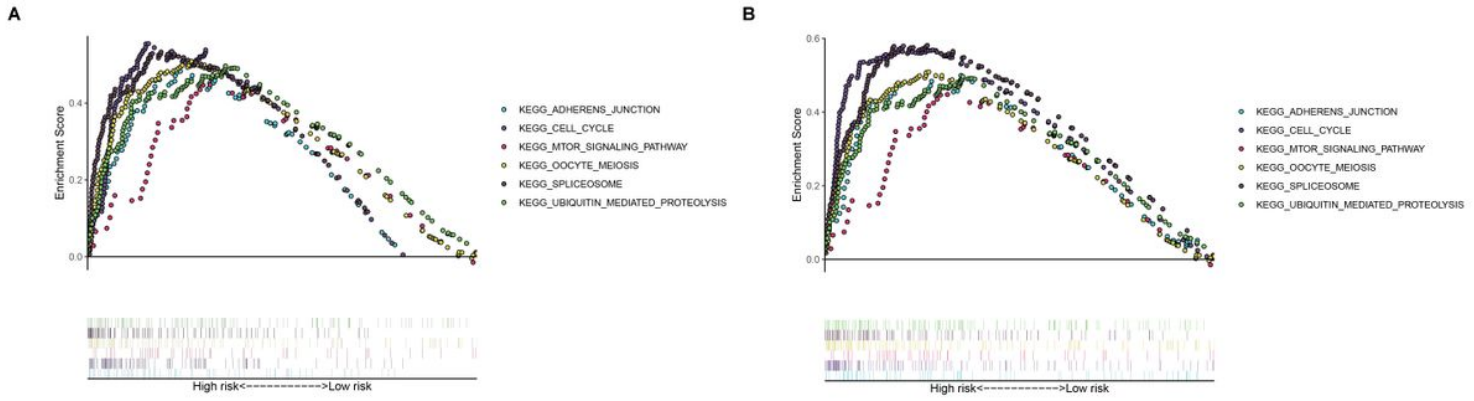

Figure 8

Gene Set Enrichment Analysis of the hypoxia risk signature in the highly risk group of TCGA (A) and ICGC (B) dataset

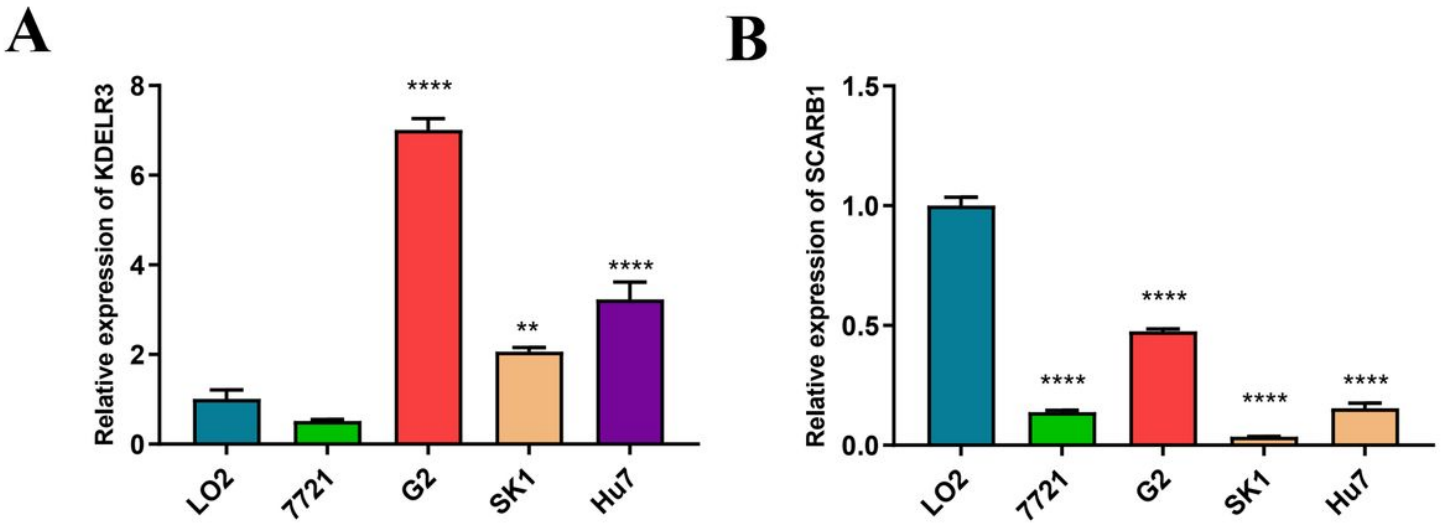

Figure 9

Relative expression of KDELR3 (A) and SCARB1 (B).7721 represent SMMC-7721,G2 represent Hep G2,SK1 represent SK-HEP-1.(*p□0.05,**p□0.0016,**** p□0.0001)

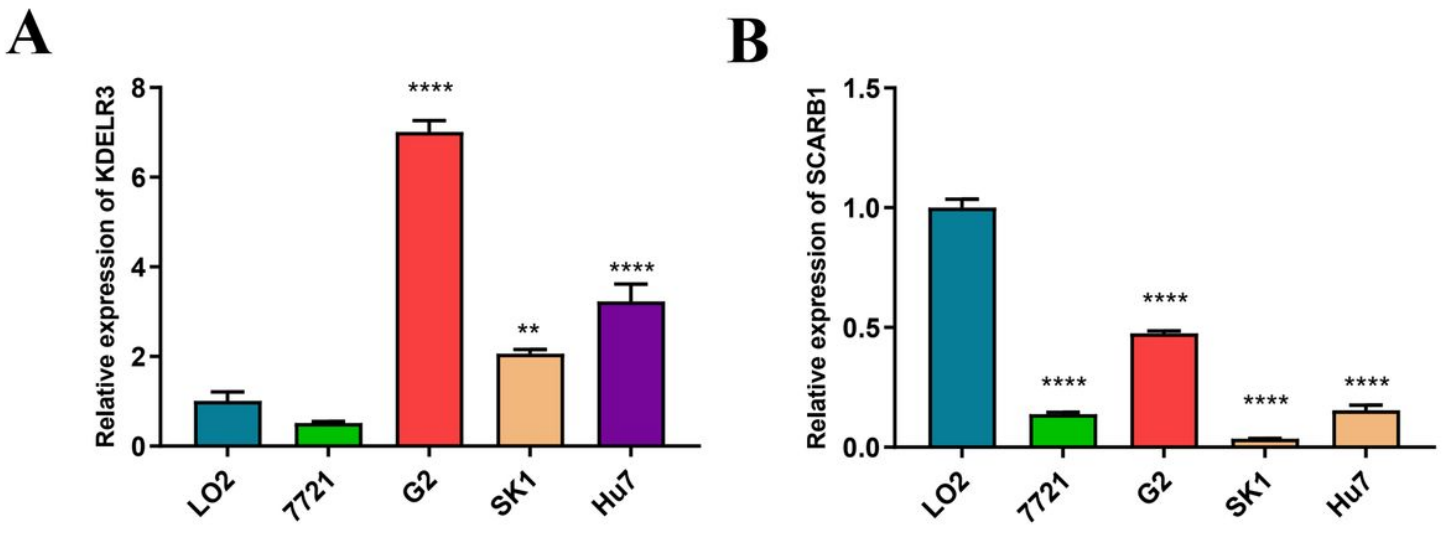

Figure 9

Relative expression of KDELR3 (A) and SCARB1 (B).7721 represent SMMC-7721,G2 represent Hep G2,SK1 represent SK-HEP-1.(*p□0.05,**p□0.0016,**** p□0.0001)